Check for updates

RESEARCH ARTICLE

JBMR®

Reduced Bone Mass and Increased Osteocyte Tartrate-Resistant Acid Phosphatase (TRAP) Activity, But Not Low Mineralized Matrix Around Osteocyte Lacunae, Are Restored After Recovery From Exogenous Hyperthyroidism in Male Mice

Eva Maria Wölfel,[1] Franziska Lademann,[2,3] Haniyeh Hemmatian,[1] Stéphane Blouin,[4,5] Phaedra Messmer,[4,5] Lorenz C. Hofbauer,[2,3] Björn Busse,[1] Martina Rauner,[2,3] Katharina Jähn-Rickert,[1,6] and Elena Tsourdi[2,3]

[1]Department of Osteology and Biomechanics, University Medical Center Hamburg-Eppendorf, Hamburg, Germany
[2]Department of Medicine III, Technische Universität Dresden Medical Center, Dresden, Germany
[3]Center for Healthy Aging, Technische Universität Dresden Medical Center, Dresden, Germany
[4]Ludwig Boltzmann Institute of Osteology at the Hanusch Hospital of OEGK and AUVA Trauma Centre Meidling, 1st Medical Department Hanusch Hospital, Vienna, Austria
[5]Vienna Bone and Growth Center, Vienna, Austria
[6]Mildred Scheel Cancer Career Center Hamburg, University Cancer Center Hamburg, University Medical Center Hamburg-Eppendorf, Hamburg, Germany

ABSTRACT

Hyperthyroidism causes secondary osteoporosis through favoring bone resorption over bone formation, leading to bone loss with elevated bone fragility. Osteocytes that reside within lacunae inside the mineralized bone matrix orchestrate the process of bone remodeling and can themselves actively resorb bone upon certain stimuli. Nevertheless, the interaction between thyroid hormones and osteocytes and the impact of hyperthyroidism on osteocyte cell function are still unknown. In a preliminary study, we analyzed bones from male C57BL/6 mice with drug-induced hyperthyroidism, which led to mild osteocytic osteolysis with 1.14-fold larger osteocyte lacunae and by 108.33% higher tartrate-resistant acid phosphatase (TRAP) activity in osteocytes of hyperthyroid mice compared to euthyroid mice. To test whether hyperthyroidism-induced bone changes are reversible, we rendered male mice hyperthyroid by adding levothyroxine into their drinking water for 4 weeks, followed by a weaning period of 4 weeks with access to normal drinking water. Hyperthyroid mice displayed cortical and trabecular bone loss due to high bone turnover, which recovered with weaning. Although canalicular number and osteocyte lacunar area were similar in euthyroid, hyperthyroid and weaned mice, the number of terminal deoxynucleotidyl transferase–mediated deoxyuridine triphosphate nick end labeling (TUNEL)-positive osteocytes was 100% lower in the weaning group compared to euthyroid mice and the osteocytic TRAP activity was eightfold higher in hyperthyroid animals. The latter, along with a 3.75% lower average mineralization around the osteocyte lacunae in trabecular bone, suggests osteocytic osteolysis activity that, however, did not result in significantly enlarged osteocyte lacunae. In conclusion, we show a recovery of bone microarchitecture and turnover after reversal of hyperthyroidism to a euthyroid state. In contrast, osteocytic osteolysis was initiated in hyperthyroidism, but its effects were not reversed after 4 weeks of weaning. Due to the vast number of osteocytes in bone, we speculate that even minor individual cell functions might contribute to altered bone quality and mineral homeostasis in the setting of hyperthyroidism-induced bone disease. © 2022 The Authors. *Journal of Bone and Mineral Research* published by Wiley Periodicals LLC on behalf of American Society for Bone and Mineral Research (ASBMR).

KEY WORDS: HYPERTHYROIDISM; OSTEOCYTIC OSTEOLYSIS; OSTEOCYTES; SECONDARY OSTEOPOROSIS; BONE MINERALIZATION

This is an open access article under the terms of the Creative Commons Attribution-NonCommercial-NoDerivs License, which permits use and distribution in any medium, provided the original work is properly cited, the use is non-commercial and no modifications or adaptations are made.

Received in original form June 3, 2022; revised form October 28, 2022; accepted November 1, 2022.

Address correspondence to: Katharina Jähn-Rickert, PhD, Department of Osteology and Biomechanics, University Medical Center Hamburg-Eppendorf, Lottestrasse 55A, 22529 Hamburg, Germany. E-mail: k.jaehn@uke.de
Elena Tsourdi, MD, Department of Medicine III & Center for Healthy Aging, Technische Universität Dresden Medical Center, Fetscherstraße 74, 01307 Dresden, Germany. E-mail: elena.tsourdi@uniklinikum-dresden.de

Additional Supporting Information may be found in the online version of this article.

EMW, FL, KJ-R, and ET contributed equally to this work.

Journal of Bone and Mineral Research, Vol. 00, No. 00, Month 2022, pp 1–13.
DOI: 10.1002/jbmr.4736

© 2022 The Authors. *Journal of Bone and Mineral Research* published by Wiley Periodicals LLC on behalf of American Society for Bone and Mineral Research (ASBMR).

15234681, 0, Downloaded from https://asbmr.onlinelibrary.wiley.com/doi/10.1002/jbmr.4736 by Sächsische Landesbibliothek, Wiley Online Library on [05/01/2023]. See the Terms and Conditions (https://onlinelibrary.wiley.com/terms-and-conditions) on Wiley Online Library for rules of use; OA articles are governed by the applicable Creative Commons License

Introduction

Secondary osteoporosis is defined as bone loss due to an underlying disease or medication. Among osteoporotic patients, up to 30% of postmenopausal women, >50% of premenopausal women, and between 50% and 80% of men suffer from secondary osteoporosis.[1] The causes are multifactorial and can include different pathologies such as endocrinological, gastroenterological, rheumatological, and hematological diseases.[1-3] One of the endocrinological diseases causing secondary osteoporosis is hyperthyroidism. Hyperthyroidism directly interferes with the bone remodeling cycle by enhancing osteoblast and osteoclast functions leading to a high bone turnover state.[4] Through favoring osteoclast-mediated bone resorption, a net bone loss is induced that contributes to elevated bone fragility.[5]

Two distinct hormones are secreted by the thyroid gland: L-thyroxine (T_4) and 3,5,3′-triiodo-L-thyronine (T_3), with T_4 levels being three to four times higher than T_3.[4] The actions of the thyroid hormones are mediated by three functional thyroid hormone receptors, namely, TRα1, TRβ1, and TRβ2, which are encoded by the *THRA* and *THRB* genes with TRα1 being predominantly expressed in the skeleton.[6] In the adult skeleton, thyroid hormones stimulate osteoblast differentiation and synthesis of the bone matrix.[7-9] In addition, osteoclastogenesis is influenced indirectly through, eg, increased expression of receptor activator of nuclear factor κB-ligand (RANKL) by thyroid hormone–stimulated cells of the osteoblast lineage.[10] Putative direct effects of thyroid hormones on osteoclastogenesis are the subject of ongoing research.[6] The actions of thyroid hormones on osteocytes remain largely unknown, although the thyroid hormone transporter Mct8 has recently been shown to be expressed in the osteocyte-like cell line MLO-Y4.[11] Distinct mouse models have been established to study the effects of thyroid hormones on bone, revealing massive trabecular bone loss and impaired bone strength due to accelerated bone turnover with drug-induced hyperthyroidism.[12,13]

Bone remodeling is controlled by osteocytes; terminally differentiated osteoblasts that residue within the mineralized bone matrix. They are interconnected via canaliculi and this lacunocanalicular network spans an area of 215 m^2 in the human skeleton.[14] When osteocytes undergo apoptosis with microcracks interrupting their network, empty osteocyte lacunae remain, and neighboring osteocytes increase RANKL secretion and by this activate osteoclasts to counteract the accumulation of damaged bone.[15] Imbalances and changes within these processes may lead to changes in bone remodeling and reduced bone quality contributing to the higher fracture susceptibility as seen in the aging skeleton.[16] In addition, osteocytes contribute to bone remodeling via the process of osteocytic osteolysis, whereby osteocytes remove nanometers of perilacunar and pericanalicular matrix within their lacunocanalicular network.[17] Especially under high bone turnover conditions, such as lactation and hyperparathyroidism, osteocytic osteolysis directly contributes to bone loss.[18,19]

In this study, we used an established mouse model of exogenously induced hyperthyroidism to evaluate whether osteocytic osteolysis also occurs during the high bone turnover state in hyperthyroidism and whether this effect is reversible through the resolution of hyperthyroidism.

Materials and Methods

Mouse model of exogenous hyperthyroidism

Animal procedures were approved by the Institutional Animal Care Committee of the Technische Universität Dresden and Landesdirektion Sachsen (TVV 2015/03). Male C57BL/6JRj mice, 12 weeks of age, were purchased from Janvier Labs (Saint Berthevin, France) and housed under institutional guidelines. Mice were fed with a standard diet, held in groups of four with 12-hour light und 12-hour dark cycles, with a cardboard house for cage enrichment purposes. Animals were controlled daily. Mice were randomized into three groups with six mice per group (control, hyperthyroidism, hyperthyroidism + weaning). Group size was determined based on previous experiments of pharmacologically induced hyperthyroidism. Hyperthyroidism was induced by adding levothyroxine (T_4; Sigma-Aldrich, Munich, Germany) to the drinking water (1.2 μg/mL) for 4 weeks as described.[12,13,20] Therefore, 6 mg/mL T_4 were dissolved in water through the addition of NaOH. The final concentration of NaOH in the drinking water was 6×10^{-7} N without changing the pH of the water. Finally, 40 μL stock solution were diluted into 200 mL of tap water. The T_4-drinking water was prepared freshly twice per week and protected from light. Following 4 weeks of T_4-drinking water, the weaning group received tap water for 4 weeks. Euthyroid mice served as control and received normal tap water. All mice had *ad libitum* access to their diet and respective drinking water. After 4 weeks T_4 treatment (hyperthyroidism group), 8 weeks of receiving tap water (control group) and 8 weeks of receiving 4 weeks T_4 and 4 weeks tap water (hyperthyroidism + weaning groups), respectively, mice were euthanized using a ketamine (100 mg/kg body weight)/xylazine solution (10 mg/kg body weight). Blood of anesthetized mice was collected by heart puncture and serum was obtained by centrifugation. Bones were collected after cervical dislocation, fixed in 4% PBS-buffered paraformaldehyde for 48 hours and stored in 50% ethanol. All subsequent analysis were performed in a blinded manner. For our preliminary analysis focusing on osteocyte changes, tibias from euthyroid and hyperthyroid mice were used from a previous study following the same treatment regimen.[12]

Three-dimensional micro–computed tomography

The distal femur and femoral midshaft were analyzed using a vivaCT 40 (Scanco Medical, Brüttisellen, Switzerland) with an X-ray energy of 70 kVp (114 mA, 200 msec integration time) and an isotropic voxel size of 10.5 μm The cortical tissue mineral density (TMD, mg HA/cm^3) and cortical thickness (Ct.Th, μm) were calculated from 100 slices at the femoral midshaft using the cortical bone evaluation program from Scanco. The trabecular tissue mineral density (TMD), the bone volume/total volume (BV/TV, %), trabecular thickness (Tb.Th, mm), trabecular separation (Tb.Sp, mm), and the trabecular number (Tb.N, 1/mm) were calculated from 100 slices starting 250 μm below and extending away from the growth plate using the Scanco bone evaluation software resulting in a volume of interest height of 1050 μm.

Serum analyses and bone turnover parameters

Serum concentrations of the bone formation marker N-terminal propeptide of type I procollagen (P1NP) and the bone resorption marker type I collagen cross-linked C-telopeptide (CTX, Ratlaps) were measured using ELISAs from IDS, Frankfurt/Main, Germany, according to the manufacturer's protocol. To assure successful experimental induction of hyperthyroidism and the resolution of the hyperthyroidism, total T_4 and total T_3 serum concentrations were measured at the end of the study using radioimmunoassays (RIA-4524 and RIA-4525 respectively; DRG

15234681, 0, Downloaded from https://asbmr.onlinelibrary.wiley.com/doi/10.1002/jbmr.4736 by Sächsische Landesbibliothek, Wiley Online Library on [05/01/2023]. See the Terms and Conditions (https://onlinelibrary.wiley.com/terms-and-conditions) on Wiley Online Library for rules of use; OA articles are governed by the applicable Creative Commons License

Instruments, Marburg, Germany). The bound radiolabeled tracer was counted in a gamma counter (1277 Gammamaster; LKB Wallac, Turku, Finland). The limit of quantification was 10nM and 0.22nM for T_4 and T_3, respectively. Intraassay coefficients of variations were below 7.5%.

Osteocyte viability

Femoral bone samples were fixed in 4% paraformaldehyde, dehydrated in an increasing ethanol series, and embedded in methylmethacrylate (MMA). Following embedding, the bone samples were cut into 4-µm-thick sections using a microtome (Leica Biosystems, Wetzlar, Germany) and stained with toluidine blue to assess osteocyte viability. Therefore, osteocytes with cell nuclei were counted in the mid-cortical bone region (at least 100 osteocytes/sample) and in the trabecular bone 1 mm below the growth plate (at least 50 osteocytes/sample) to obtain the number of viable osteocytes over the analyzed bone area (N.Ot/B.Ar, 1/mm^2) and the number of osteocyte lacunae without cell nuclei over analyzed bone area (N.eLc/B.Ar, 1/mm^2). Finally, the percentage of nuclei-empty osteocyte lacunae were calculated by dividing the number of empty lacunae by the total number of osteocyte lacunae (N.eLc/Tt.Lc, %). Analysis was performed using the Osteomeasure software (OsteoMetrics, Decatur, GA, USA).

By performing a terminal deoxynucleotidyl transferase–mediated deoxyuridine triphosphate nick end labeling (TUNEL) assay, osteocyte viability was assessed on the bone sections using an In Situ CellDeathDetection Kit (Roche Diagnostics, Mannheim, Germany) according to the manufacturer's instructions. The percentage of TUNEL-positive osteocytes over total osteocyte number (TUNEL+ Ot, %) was determined in the mid-cortical bone region and in the trabecular bone 1 mm below the growth plate.

Osteocyte canaliculi evaluation

For osteocyte canaliculi evaluation, 4-µm sections of femoral bone embedded in MMA were stained using Ploton's silver nitrate precipitation[21] with a thionine counter staining.[22] By this, the osteocyte canaliculi become visible and allow to assess two-dimensional (2D) canalicular number (Ot.Ca/Lc). Furthermore, the osteocyte lacunar area was assessed to normalize the canaliculi per osteocyte lacunar area (Ot.Ca/Lc.Ar, 1/µm^2). Compartment-specific analyses were performed in the mid-cortical bone region for cortical analysis and in the trabecular compartment 1 mm below the growth plate. Per sample and region 15 osteocyte lacunae were evaluated.

Quantitative backscattered electron imaging

To assess the mineralization degree and for analyses of the 2D osteocyte lacunar area, quantitative backscattered electron imaging (qBEI) was performed. The MMA-embedded femoral bone samples were grinded to a co-planar state and polished on the bone surface using 1200 silicon/carbide paper. The samples were sputtered with carbon and mounted into a vacuum chamber of a scanning electron microscope system (LEO 435 VP; LEO Electron Microscopy Ltd., Cambridge, England). Using a backscattered electron detector (Type 202; K.E. Developments Ltd., Cambridge, England) with constant working distance of 20 mm, constant voltage of 20 kV, and constant beam current of 680 pA, images were taken at magnification ×150 resulting in 0.74 µm resolution. Using a calibration standard with aluminum and carbon, grayscale images were obtained, which are used to determine the mineralization degree based on calcium weight percentage.[23]

2D osteocyte lacuna evaluation

To analyze osteocyte lacunar area, qBEI images were taken in a standardized manner from the longitudinal mid-section bone surface. For tibial specimens: (i) cortical bone was captured at 1 mm length at midshaft on both cortices resulting in 100–150 lacunae per specimen, and (ii) trabecular bone was captured in an image area of 0.25 mm^2 starting 1 mm below the proximal growth plate resulting in 50–75 lacunae per specimen. For femoral specimens: (i) cortical bone was captured at 0.75 mm length at midshaft on both cortices resulting in 100–200 lacunae per specimen, and (ii) trabecular bone was captured in an image area of 0.7 mm^2 starting 1 mm below the distal growth plate resulting in 50–100 lacunae per specimen. Quantitation to assess osteocyte lacunar area (Lc.Ar, µm^2) was done using ImageJ Software (NIH, Bethesda, MD, USA; https://imagej.nih.gov/ij/) with a lower size limit of 10 µm^2 and an upper size limit of 250 µm^2. A gray-level threshold was determined and set to 90, reflecting the mineralized bone matrix over nonmineralized regions within representative specimens from all groups. Additionally, 2D osteocyte lacunae section analyses were extended to frontal sections of three lumbar vertebra and corresponding one transversal section of midshaft femur in six controls and seven T_4-treated animals (Fig. S1). For this time a scanning electron microscope with a field emission cathode (SUPRA 40; Carl Zeiss AG, Oberkochen, Germany) working at 20 kV energy, 10 mm working distance and 280–320-pA probe current was used. Images were taken with 0.88 µm spatial resolution. The osteocytes lacunae areas were discriminated from mineralized bone matrix using a gray-level threshold of 55 corresponding to 5.2% wt Ca and a size range 3–80 µm^2. For vertebral and femoral cross-sectional analysis of osteocyte area, the entire frontal vertebral cut and the entire femoral cross section were imaged resulting in, respectively, (i) 999 ± 476 and (ii) 715 ± 68 lacunae analyzed per specimen.

Three-dimensional osteocyte lacuna evaluation

Femoral samples embedded in MMA were scanned using a high-resolution desktop micro–computed tomography (µCT) (Skyscan 1272; Bruker, Kontich, Belgium) at a voxel size of 0.7 µm, 40 kV acceleration voltage, 230 µA tube current, 5185 ms exposure time, and 0.2-degree rotation step to access three-dimensional (3D) osteocyte lacunar morphology. A length of 1.4 mm of the distal metaphysis starting 1 mm above the growth plate was scanned. Postprocessing was performed using our reported technique.[24] Briefly, after applying Otsu thresholding, the osteocyte lacunar network was segmented using the 3D despeckle filter in CTAn (Bruker, Kontich, Belgium). Objects with volumes between 100 and 1500 µm^3 were assumed to be osteocyte lacunae. Following segmentation, the volume of each individual osteocyte lacuna was determined.

Mineralization degree evaluation

Postprocessing to determine the bone mineral density distribution was done using a customized Matlab script (MATLAB R2014a; MathWorks, Natick, MA, USA). By this, the following parameters were assessed: (i) the average calcium weight percentage presented as calcium mean (CaMean, wt%), (ii) the peak

15234681, 0, Downloaded from https://asbmr.onlinelibrary.wiley.com/doi/10.1002/jbmr.4736 by Sächsische Landesbibliothek, Wiley Online Library on [05/01/2023]. See the Terms and Conditions (https://onlinelibrary.wiley.com/terms-and-conditions) on Wiley Online Library for rules of use; OA articles are governed by the applicable Creative Commons License

position in the histogram, the most frequently measured calcium weight percentage (CaPeak, wt%), (iii) the heterogeneity of the mineralization expressed as the standard deviation of the calcium distribution curve (CaWidth, wt%), (iv) the percentage bone area which is lower than the 5th percentile value of the reference histogram (CaLow,% bone area), and (v) the percentage bone area which is higher mineralized than the 95th percentile value of the reference histogram (CaHigh, % bone area). Images were obtained for both regions, the trabecular region 1 mm below the growth plate and the mid-cortical region of the longitudinal sectioned femoral areas.

To determine the mineralization degree around the osteocyte lacunae in the trabecular region, a 2500-μm^2 quadrant around each lacuna was selected and evaluated to determine the above-mentioned parameters directly around the osteocyte lacuna and to assess potential demineralization of the matrix surrounding the osteocyte lacunae as sign of osteocytic osteolysis. If more than one osteocyte lacuna was within the selected quadrant, the second osteocyte lacuna was not measured again to avoid measuring the same region twice.

Tartrate-resistant acid phosphatase staining

For the tartrate-resistant acid phosphatase (TRAP) staining, paraffin sections from tibiae and femurs were dewaxed, rehydrated, and stained for TRAP activity as described.[13] Histomorphometry was performed to determine osteoclast (N.Oc/B.Pm, 1/mm: Oc.S/BS, %) and osteoblast (N.Ob/B.Pm, 1/mm; Ob.S/BS, %) indices. To evaluate the amount of TRAP+ osteocytes, one to 200 osteocytes were analyzed, and TRAP-positive osteocytes were determined both in trabecular and cortical bone in a blinded fashion.[17] TRAP-positive osteocytes were normalized to total number of osteocytes (TRAP+ Ot, %).

Statistical analysis

For a priori sample size calculation, GPower 3.1 was used. Data were tested for normality using Kolmogorov-Smirnov test. In our preliminary analysis, we compared two groups using Student's *t* test. The three groups, euthyroid, hyperthyroid, and weaning, were compared using one-way ANOVA for normally distributed data with Tukey's multiple comparisons test and Kruskal-Wallis test for non-normally distributed data. Outliers were identified using Grubbs' test implemented in the statistics software. An α-level of 0.05 was defined as statistically significant. Statistical analysis was performed using GraphPad Prism 9.1.2 (GraphPad Software, Inc., La Jolla, CA, USA). All data are presented as median $\pm$ interquartile range in the figures and as mean $\pm$ standard deviation (SD) within the text.

Results

Mild enlargement of osteocyte lacunae detected in a mouse model of exogenous hyperthyroidism

We have previously reported on the low bone mass phenotype, along with prominent osteoclast activity in a validated male C57BL/6 mouse model of T_4-induced hyperthyroidism.[12] When examining the histological sections, also a higher TRAP-positivity of osteocytes became apparent (Fig. 1*A*). Addition of T_4 to the drinking water led to a significantly higher number of TRAP-positive osteocytes within both bone compartments compared to euthyroid mice (Fig. 1*B*). In the cortical bone compartment, the results did not change when one detected outlier in T_4 group was removed (adjusted *p*-value < 0.0001). The qBEI-based 2D quantification in cortical and trabecular bone compartments determined a mildly but significantly enlarged osteocyte lacunar area in tibial bone of hyperthyroid mice compared to euthyroid mice (Fig. 1*C,D*) shown by a 10.99% and 13.76% larger osteocyte lacunar area, respectively.

Reversible T_4-induced cortical and trabecular bone loss

One major characteristic of lactation-induced osteocytic osteolysis is its reversibility with weaning.[17] In accordance, we set out to investigate whether T_4-induced osteocytic osteolysis is reversible and therefore established a T_4-weaning model. µCT analysis revealed trabecular and cortical bone loss with hyperthyroidism which recovered in the weaning group (Fig. 2*A*). Cortical thickness and tissue mineral density were recovered with weaning from T_4, whereas cortical thickness was 7.85% lower in hyperthyroid femurs compared to euthyroid (Fig. 2*B*). Differences in TMD remained after removal of one outlier in the weaning group (We group) (adjusted *p*-value = 0.0098). Similar effects were also seen in the trabecular bone volume fraction with decreased Tb. BV/TV in the T_4 group compared to the euthyroid and weaning group (Fig. 2*C*). Further, we determined a reduced trabecular thickness in T_4-treated mice as compared to weaned, but not euthyroid animals (Fig. 2*D*). Trabecular number was 23.67% lower with T_4 and remained 17.06% lower post-T_4 exposure, both compared to euthyroid (Fig. 2*D*). Together this resulted in an increased trabecular separation in hyperthyroid mice compared to weaned (Fig. 2*D*) and euthyroid animals.

T_4-induced elevated bone remodeling is normalized with weaning

With regard to bone resorption, CTX concentrations were increased in hyperthyroid animals compared to their euthyroid counterparts, which was normalized to the euthyroid level upon weaning (Fig. 3*A*). Differences remained after removal of one outlier in the T_4 group (adjusted *p*-values < 0.0001 for both comparisons). We confirmed that bone resorption recovered during weaning as osteoclast parameters, ie, number of osteoclasts and osteoclast surface were reduced in the weaning group as compared to T_4-treated mice (Fig. 3*B,C*). Enhanced bone formation with T_4 was shown by an elevated serum level of P1NP as compared to euthyroid mice (Fig. 3*C*) that normalized upon weaning to the euthyroid level (Fig. 3*D*). In accordance, number of osteoblasts and osteoblast surface were highest in the T_4 group compared to euthyroid and weaned mice (Fig. 3*C,E*).

The osteocyte network is unaffected by T_4 and weaning

When osteocytes undergo cell death, eg, via apoptosis, an empty lacuna may be left behind within the bone matrix. In cortical bone, the number of osteocyte lacunae as well as the percentage of empty lacunae over total lacunar number were unaffected and no differences were seen between the three groups (Fig. 4*A*). However, the percentage of apoptotic osteocytes in the cortex was lowest with weaning compared to euthyroid mice (Fig. 4*B*). In the trabecular compartment, osteocyte viability was similar between all three groups and no significant changes were induced by neither T_4 nor weaning (Fig. 4*C,D*). Based on Ploton silver precipitation, canaliculi were evaluated as part of the osteocyte lacunocanalicular network contributing to network connectivity. Canaliculi per lacuna were determined in 2D in cortical and trabecular bone (Fig. 4*E,F*). In both compartments,

15234681, 0, Downloaded from https://asbmr.onlinelibrary.wiley.com/doi/10.1002/jbmr.4736 by Sächsische Landesbibliothek, Wiley Online Library on [05/01/2023]. See the Terms and Conditions (https://onlinelibrary.wiley.com/terms-and-conditions) on Wiley Online Library for rules of use; OA articles are governed by the applicable Creative Commons License

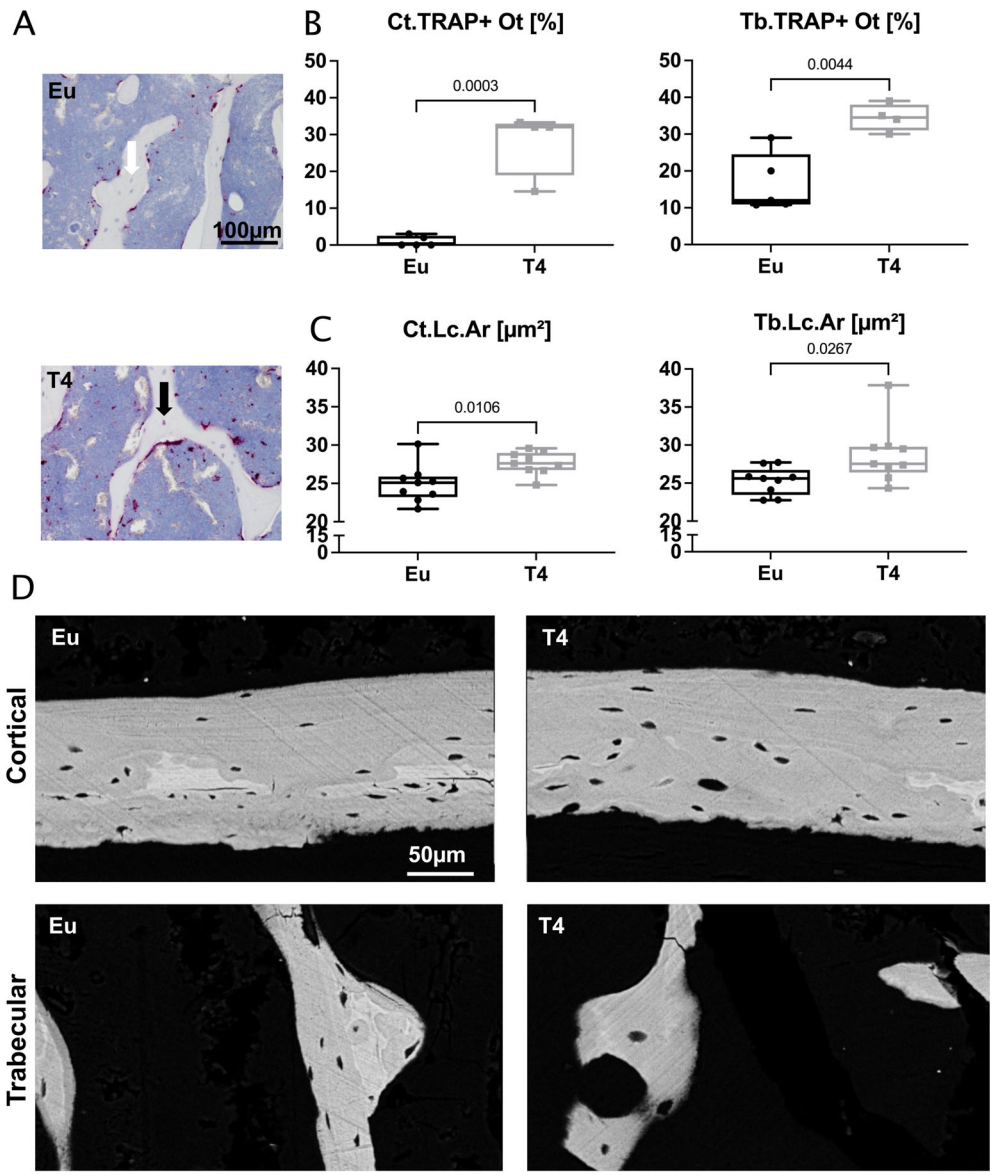

Fig. 1. Mild osteocytic osteolysis is induced by levothyroxine (T_4) treatment. Twelve-week-old male mice were rendered hyperthyroid by adding T_4 to the drinking water over 4 weeks or received tap water as control. (*A*). TRAP activity staining was performed on histological sections from tibial midshafts of Eu and T4 mice (Eu $n = 5$, T4 $n = 4$). The white arrow indicates an example of a TRAP-negative osteocyte while the black arrow points at a TRAP-positive osteocyte. (*B*) Quantification of TRAP-positive osteocytes in femoral cortical (Ct.TRAP+ Ot) and vertebral trabecular bone (Tb.TRAP+ Ot). (*C*) Using qBEI, the 2D osteocyte lacunar area was evaluated in cortical bone (Ct.Lc.Ar) and trabecular bone (Tb.Lc.Ar) ($n = 9$ for both groups). (*D*) Representative qBEI images of osteocyte lacunae in cortical and trabecular bone of Eu and T4 mice. Box plots show median line and the 25th and 75th percentile, the error bars represent the minimum (0th percentile) and the maximum (100th percentile). Individual data points are shown as dots. Statistical analysis was performed using an unpaired Student's *t* test and $p < 0.05$ was considered significant. Eu = euthyroid control group; T4 = hyperthyroid group.

the number of canaliculi per lacuna was similar between all three groups and thus, not affected by neither T_4 nor weaning (Fig. 4*G*). Additionally, we did not detect any significant changes in the percentage of apoptotic osteocytes (Fig. 4*H*), which remained after removal of one outlier in Eu and T_4 groups.

Early state of T_4-induced mild osteocytic osteolysis recovered with weaning

Although we previously detected a mild but significant effect on lacunar area both in cortical and trabecular bone as shown in Fig. 1, this experimental setup did not reveal a difference in lacunar area (Fig. 5*A*). Although one outlier in the T_4 group was detected, removal of this outlier did not change the results. However, we reproduced the finding of 8.2-fold higher TRAP activity with T_4 compared to euthyroid that was fully reversed to the euthyroid level with weaning (Fig. 5*B*), which was unchanged upon removal of one outlier in Eu and T_4 group (adjusted *p*-value = 0.0011 for Eu versus T4 and adjusted *p*-value = 0.0113 for T_4 versus We). The additional measurement in femoral transversal and vertebral frontal sections did also not detect any differences between Eu and T_4 mice. However, the lacunar areas

15234681, 0, Downloaded from https://asbmr.onlinelibrary.wiley.com/doi/10.1002/jbmr.4736 by Sächsische Landesbibliothek, Wiley Online Library on [05/01/2023]. See the Terms and Conditions (https://onlinelibrary.wiley.com/terms-and-conditions) on Wiley Online Library for rules of use; OA articles are governed by the applicable Creative Commons License

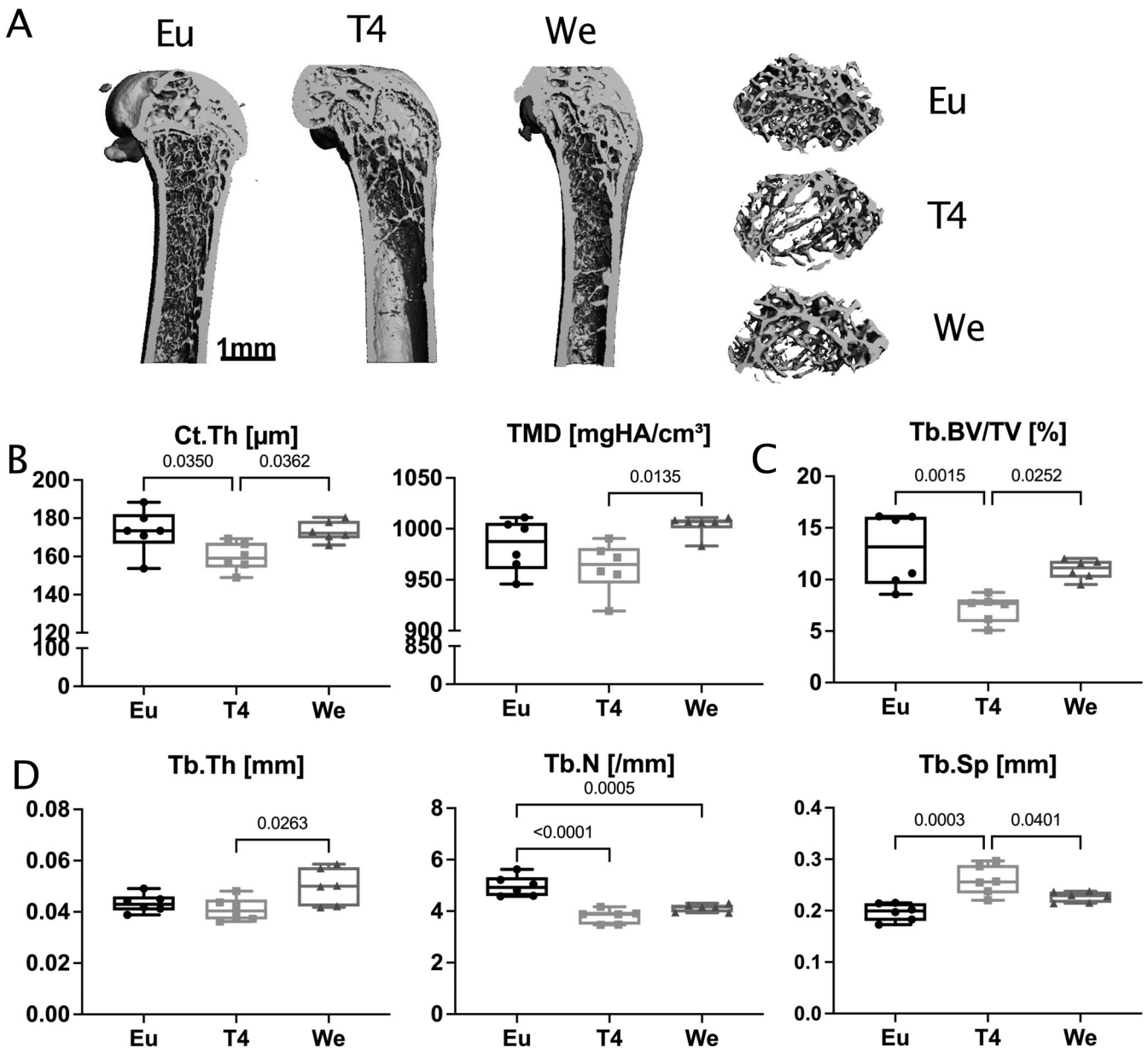

Fig. 2. Reversible T_4-induced cortical and trabecular bone loss. Twelve-week-old male mice were rendered hyperthyroid by adding T_4 to the drinking water over 4 weeks or received tap water as control. Following 4 weeks of T_4-drinking water, the weaning group received tap water for 4 weeks. High-resolution µCT was performed on femurs from Eu, T4, and We mice ($n = 6$ per group). (*A*) Representative images of 3D reconstructions. (*B*) Cortical thickness (Ct.Th) and tissue mineral density (TMD) of the cortex. (*C*) Trabecular bone volume fraction (Tb.BV/TV). (*D*) Trabecular thickness (Tb.Th), number of trabeculae (Tb.N) and trabecular separation (Tb.Sp). Box plots show median line and the 25th and 75th percentile, the error bars represent the minimum (0th percentile) and the maximum (100th percentile). Individual data points are shown as dots. Statistical analysis was performed using one-way ANOVA with Tukey post hoc test and $p < 0.05$ was considered significant. Eu = euthyroid control group; T4 = hyperthyroid group; We = weaning group.

in trabecular bone were larger than in cortical bone of Eu mice (Fig. S1). This difference is preserved with T_4 treatment (Fig. S1). Variations in the threshold for osteocyte lacunar section (OLS) size and gray levels for discrimination between mineralized matrix and lacunae influenced the absolute OLS parameter values but did not affect our conclusions (Fig. S2).

In the trabecular bone compartment larger lacunae with >250 µm^3 were more prominent in the hyperthyroid compared to the euthyroid group. However, this was also the case in the weaning group (Fig. 5*C*,*D*).

Lower local trabecular calcium content suggests early signs of osteocytic osteolysis in hyperthyroidism

Based on calcium weight percentages, the mineral density distribution was determined using qBEI (Fig. 6*A*). In the trabecular region, we found a clear shift of the bone mineral density distribution curves toward lower calcium weight percentages in the T_4 and the weaning group (Fig. 6*B*), reproducing our previous findings in hyperthyroid mice.[13] This is also shown by a tendency toward a lower calcium mean in the hyperthyroid group

15234681, 0, Downloaded from https://asbmr.onlinelibrary.wiley.com/doi/10.1002/jbmr.4736 by Sächsische Landesbibliothek, Wiley Online Library on [05/01/2023]. See the Terms and Conditions (https://onlinelibrary.wiley.com/terms-and-conditions) on Wiley Online Library for rules of use; OA articles are governed by the applicable Creative Commons License

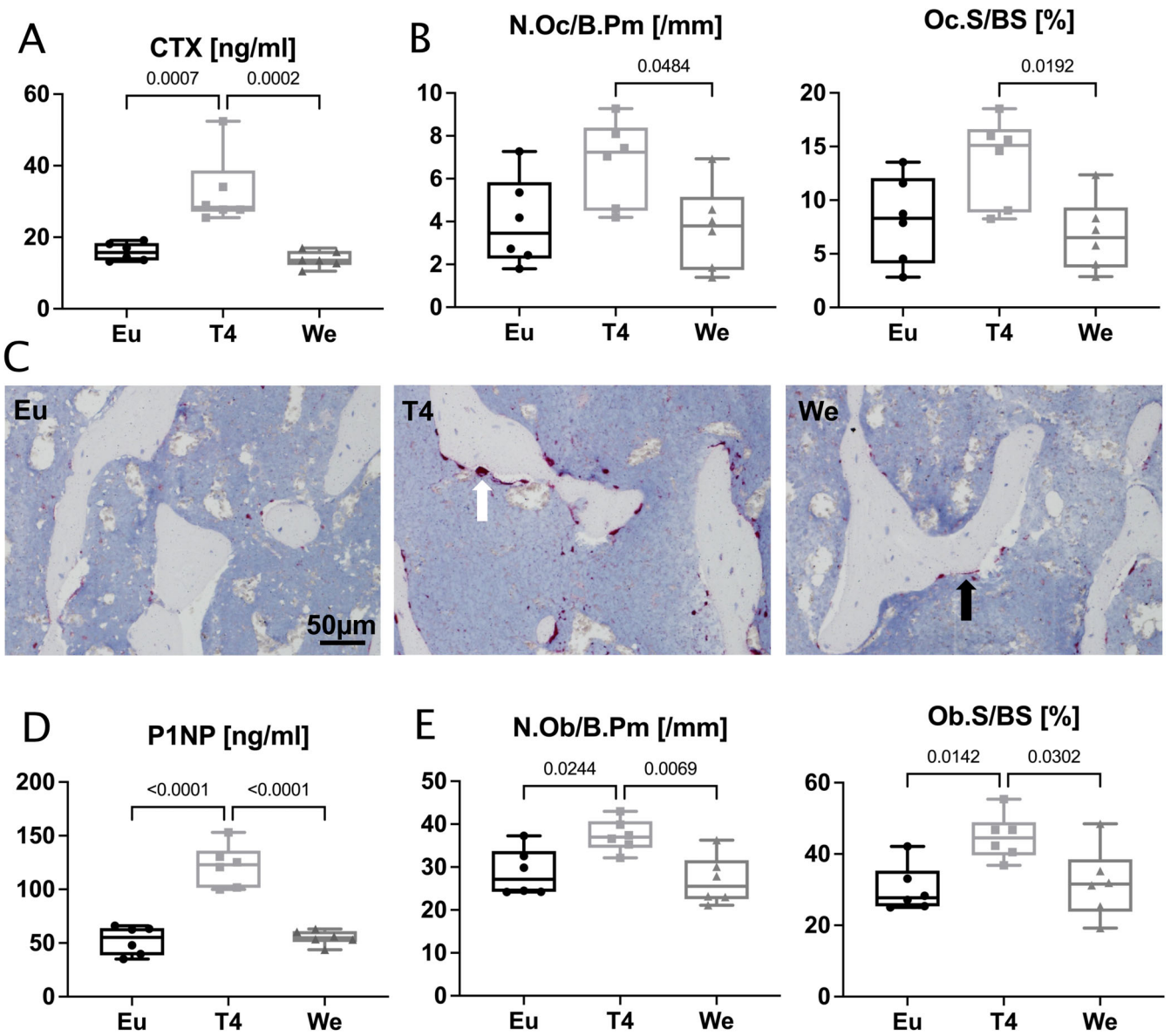

Fig. 3. T_4-induced high bone turnover is normalized after weaning. (*A*) Bone resorption marker C-terminal telopeptide of type I collagen (CTX) was measured in serum of Eu, T4, and We mice. Based on TRAP staining, (*B*) trabecular bone resorption in femurs was determined via number of osteoclasts per bone perimeter (N.Oc/B.Pm) and osteoclast surface per bone surface (Oc.S/BS). (*C*) the bone formation serum marker N-terminal propeptide of type I collagen (P1NP) was measured in serum samples using an ELISA. (*D*) Number of osteoblasts per bone perimeter (N.Ob/B.Pm) and osteoblast surface per bone surface (Ob.S/BS) were assessed in histological sections. (*E*) Representative images of TRAP stained trabecular bone in Eu, T4, and We groups. White arrow indicating an osteoclast and black arrow pointing at osteoblasts. $n = 6$ per group. Box plots show median line and the 25th and 75th percentile, the error bars represent the minimum (0th percentile) and the maximum (100th percentile). Individual data points are shown as dots. Statistical analysis was performed using one-way ANOVA with Tukey post hoc test and $p < 0.05$ was considered significant. Eu = euthyroid control group; T4 = hyperthyroid group; We = weaning group.

compared to the euthyroid group, which did not reach a significant difference (Fig. 6*C*). However, upon removal of one detected outlier in the Eu group, the T_4 and We group presented with significantly lower CaMean values compared to the Eu group (adjusted p-value = 0.0034 and adjusted p-value = 0.0055, respectively). The peak position of Ca wt% (CaPeak) was 2.55% lower in hyperthyroid compared to the euthyroid group, with a similar trend in the weaning group compared to the euthyroid group. The heterogeneity (CaWidth) along with the percentage of bone area with low (CaLow) or high (CaHigh) mineralized bone packets was similar between all three groups. In the cortical midshaft region, the above specified mineralization parameters were not significantly different between the groups (Fig. S3).

Osteocytic osteolysis includes acidic removal of mineral from the perilacunar matrix of osteocytes.[25] Here, we observed a 2.74% lower average calcium wt% directly around the lacuna in T_4 compared to euthyroid mice (Fig. 6*D*), which did not recover in the weaning group as shown by a significantly lower value

15234681, 0, Downloaded from https://asbmr.onlinelibrary.wiley.com/doi/10.1002/jbmr.4736 by Sächsische Landesbibliothek, Wiley Online Library on [05/01/2023]. See the Terms and Conditions (https://onlinelibrary.wiley.com/terms-and-conditions) on Wiley Online Library for rules of use; OA articles are governed by the applicable Creative Commons License

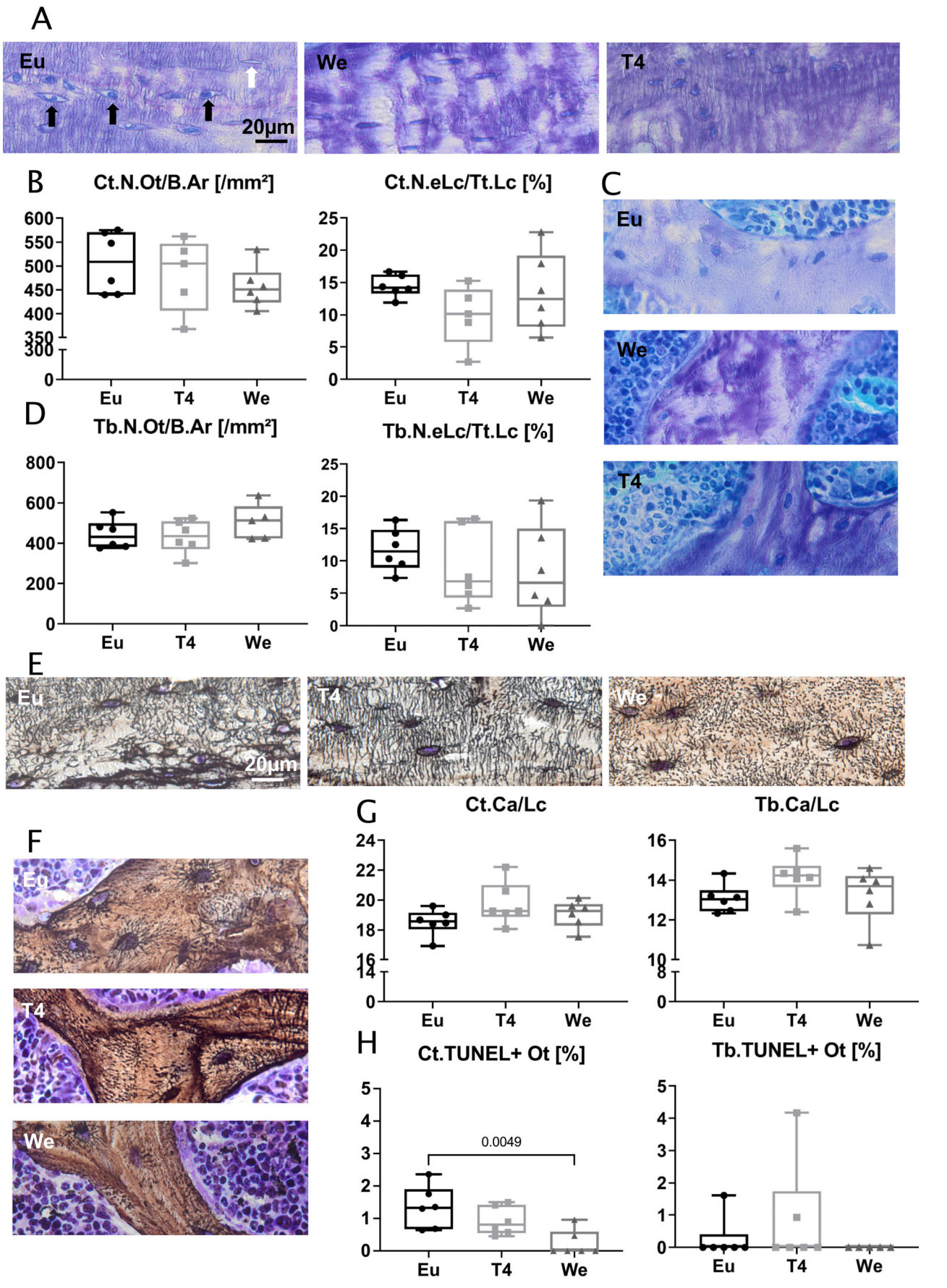

(Figure legend continues on next page.)

15234681, 0, Downloaded from https://asbmr.onlinelibrary.wiley.com/doi/10.1002/jbmr.4736 by Sächsische Landesbibliothek, Wiley Online Library on [05/01/2023]. See the Terms and Conditions (https://onlinelibrary.wiley.com/terms-and-conditions) on Wiley Online Library for rules of use; OA articles are governed by the applicable Creative Commons License

compared to euthyroid. Results remained after removal of one outlier in the Eu group (adjusted p-value = 0.005 Eu versus T4 and adjusted p-value = 0.004 Eu versus We). In contrast, calcium peak and calcium width were similar between the three groups (Fig. 6E), which did not change after removal of one outlier in the Eu group for calcium peak.

Discussion

In this study, we analyzed bones from euthyroid mice, hyperthyroid mice, and mice treated with T_4 followed by a weaning period of 4 weeks that allowed for monitoring transient changes in osteocyte physiology and bone quality during hyperthyroidism and its recovery to a euthyroid state. Here, we found evidence for osteolytic activity of osteocytes after 4 weeks of T_4 administration in mice, which was still present 4 weeks post T_4 administration in terms of remaining lower perilacunar mineralization. Although cortical and trabecular bone mass recovered with weaning due to a normalization in bone remodeling activities by osteoclasts and osteoblasts, the persistently decreased local bone mineralization around osteocyte lacunae indicates altered local bone quality.

In our previous study, we initially investigated bone of euthyroid versus hyperthyroid-rendered mice.[12] We determined a robust activity of TRAP, not solely in osteoclasts, but also in trabecular and cortical osteocytes upon T_4 administration in the load-bearing tibia. TRAP is considered a classical bone turnover marker and in patient sera reflects the number of active osteoclasts.[26] As a metalloenzyme, TRAP may catalyze the hydrolysis of phosphate esters and anhydrides under acidic conditions. As for osteocytes, TRAP activity has been described in the past,[27] but has more recently been attributed to the process of osteocytic osteolysis.[25]

Following these results, we posed the question of whether osteocytic bone resorption in hyperthyroidism would be reversible upon return to the euthyroid state. Therefore, we undertook an additional set of experiments, including a 4-week weaning group. Here we saw a complete normalization of cortical thickness and a higher tissue mineral density as compared to the hyperthyroid group, suggesting that both cortical bone mass and hydroxyapatite content were restored within 4 weeks of weaning. Interestingly, in the trabecular compartment, the effect on trabecular thickness and overall bone volume fraction suggested a positive balance of bone remodeling favoring bone formation during weaning. However, trabecular number was not yet restored within 4 weeks post T_4-exposure, suggesting a differential effect of bone turnover activities in the individual bone compartments. In hyperthyroid patients, a reversibility of bone mineral density loss was reported after 1 year radioiodine therapy.[28] Additionally, bone loss induced by thyroid hormone excess was shown to be reversible with thyreostatic therapy.[29] Although some authors detected normalized bone mineral density values after 3–6 years of treatment,[30] others determined an incomplete reversibility at earlier time points.[31]

Both serological and histological osteoblast and osteoclast parameters revealed a complete reversal of the high bone turnover state due to hyperthyroidism in trabecular bone after weaning. Data from hyperthyroid patients show similarly elevated levels of bone turnover makers that return to normal levels upon resolution of hyperthyroidism.[32] Despite that we could not determine a significant effect on 2D or 3D lacunar size, results of cellular activity and local bone mineralization analyses because contributors to bone quality showed signs of osteocytic osteolysis. Interestingly, we observed a complete recovery of the number of TRAP-positive osteocytes upon weaning from hyperthyroidism. Mineralization analysis showed a significantly lower calcium content with hyperthyroidism around the osteocyte lacunae including the perilacunar matrix, which did not return to euthyroid levels after weaning. The most pronounced effects on lacunar enlargement were previously shown within the lactation model of CD1 mice, but also in C57BL/6 mice that were either selected for sufficient litter size or fed with a low calcium diet to increase the need for calcium release through osteolysis.[25] However, others have not determined effects on lacunar size,[33] or required the addition of a potent external stimuli such as lactation.[34] In comparison to a 12-day-lactation 7-day-weaning regime including a complete recovery of the TRAP-positive osteocytes within larger osteocyte lacunae,[25] the mouse model of hyperthyroidism utilizes the established 4-week T_4-administration and a 4-week weaning period. Thus, differences between the two models could be due to the fact that the time point for detection of osteocytic osteolysis was potentially not optimal in the model of hyperthyroidism and a shorter T_4 exposure should be considered.

The potential controversy of osteocytic osteolysis has been based on focusing solely on lacunar enlargement,[35] which neglects the number of osteocytes and their active surface volume.[14] However, additional parameters involving lacunar acidification and proteolytic degradation are considered to additionally describe osteocytic osteolysis.[17,25] Perilacunar remodeling has been previously presented in the absence of changes in osteocyte lacunar size, based on markers such as Cathepsin K or TRAP in osteocytes.[33,34] Although we could only find a small but significant effect on lacunar size comparing hyperthyroid with euthyroid mice with a larger n-number of animals, this effect diminished when adding an additional group (Weaning) and decreasing animal number. However, we could

(Figure legend continued from previous page.)

Fig. 4. The osteocyte network is unaffected by hyperthyroidism and weaning. Osteocyte viability in Eu, T4, and We mice was investigated on femoral bone sections ($n = 6$ per group). Toluidine blue histology was performed to quantify osteocyte-inhabited lacunae versus empty osteocyte lacunae. TUNEL assay determined the percentage of currently apoptotic cells in the consecutive sections. Representative images are shown for each staining. In *A*, cortical bone was quantified regarding osteocyte lacunar number per bone area (N.Ot/B.Ar), and percentage of empty lacunae over total number of lacunae (N.eLc./Tt.Lc) in *B*. In trabecular bone in *C*, the same indices were assessed in *D*. In both bone compartments, cortical bone in *E* and trabecular bone in *F*, canalicular numbers (Ca/Lc) were determined in Ploton silver precipitated sections in *G*. (*H*) The percentage of apoptotic osteocytes (TUNEL+ Ot) were quantified in cortical bone (Ct.) and trabecular bone (Tb.). Box plots show median line and the 25th and 75th percentile, the error bars represent the minimum (0th percentile) and the maximum (100th percentile). Individual data points are shown as dots. Statistical analysis was performed using one-way ANOVA with Tukey post hoc test and $p < .05$ was considered significant. Eu = euthyroid control group; T4 = hyperthyroid group; We = weaning group.

15234681, 0, Downloaded from https://asbmr.onlinelibrary.wiley.com/doi/10.1002/jbmr.4736 by Sächsische Landesbibliothek, Wiley Online Library on [05/01/2023]. See the Terms and Conditions (https://onlinelibrary.wiley.com/terms-and-conditions) on Wiley Online Library for rules of use; OA articles are governed by the applicable Creative Commons License

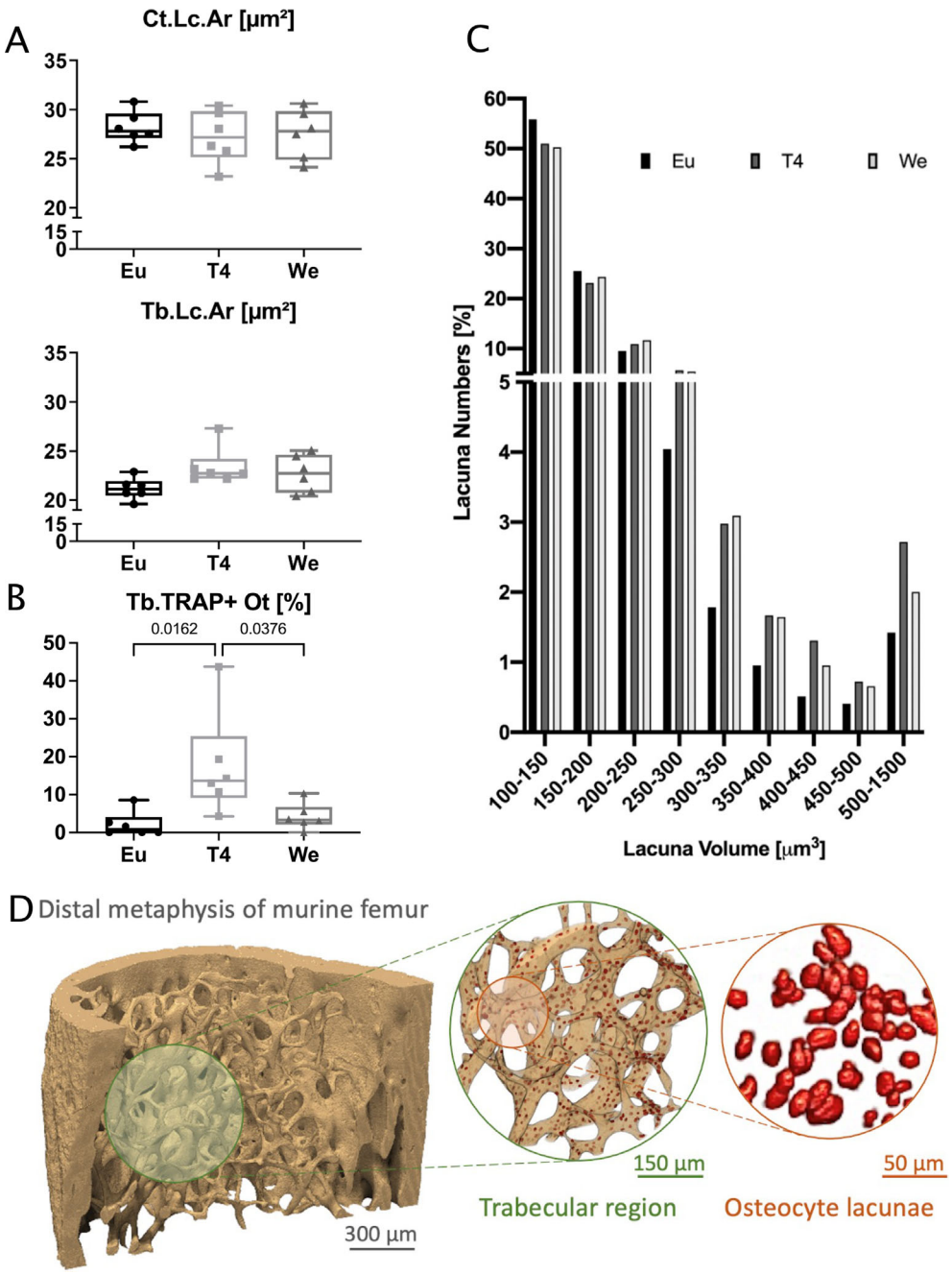

Fig. 5. No recovery from thyroid hormone–induced mild osteocytic osteolysis with weaning. (*A*) Lacunar area (lc.Ar) in femurs of Eu, T4, and We animals was determined on backscattered electron microscopy images in cortical (Ct.) and trabecular (Tb.) bone ($n = 6$ per group). (*B*) TRAP-positive osteocytes were counted in the femoral trabecular bone compartment (Tb.TRAP+ Ot). (*C*) High-resolution µCT analysis–based quantification of lacunar volume over lacuna number ($n = 3$ per group). (*D*) Representative µCT images of the osteocyte lacunae in the trabecular bone compartment. Box plots show median line and the 25th and 75th percentile, the error bars represent the minimum (0th percentile) and the maximum (100th percentile). Individual data points are shown as dots. Statistical analysis was performed using one-way ANOVA with Tukey post hoc test and $p < 0.05$ was considered significant. Eu = euthyroid control group; T4 = hyperthyroid group; We = weaning group.

find indications of osteocytic osteolysis based on higher TRAP activity in osteocytes and lower mineralization around osteocyte lacunae. Due to the large network that osteocytes span, resulting in an impressive active surface volume, even small changes in osteocyte lacunar activity may impair bone quality. Although an earlier time point for analysis of osteocytic osteolysis (eg, 14 days of T_4 treatment followed by 7 days of recovery) might allow for detection of larger differences regarding osteocyte properties, shorter time points might weaken the bone phenotype of the established hyperthyroid mouse model used, which is dependent on treatment time.

15234681, 0, Downloaded from https://asbmr.onlinelibrary.wiley.com/doi/10.1002/jbmr.4736 by Sächsische Landesbibliothek, Wiley Online Library on [05/01/2023]. See the Terms and Conditions (https://onlinelibrary.wiley.com/terms-and-conditions) on Wiley Online Library for rules of use; OA articles are governed by the applicable Creative Commons License

Because osteocyte properties and mineralization degree both contribute to bone quality, we further analyzed the global trabecular calcium content, which was presented with a significantly lower calcium peak in T_4 compared to euthyroid mice. The weaning group did not show any statistical differences but showed similar mean values to the T_4 group indicating an

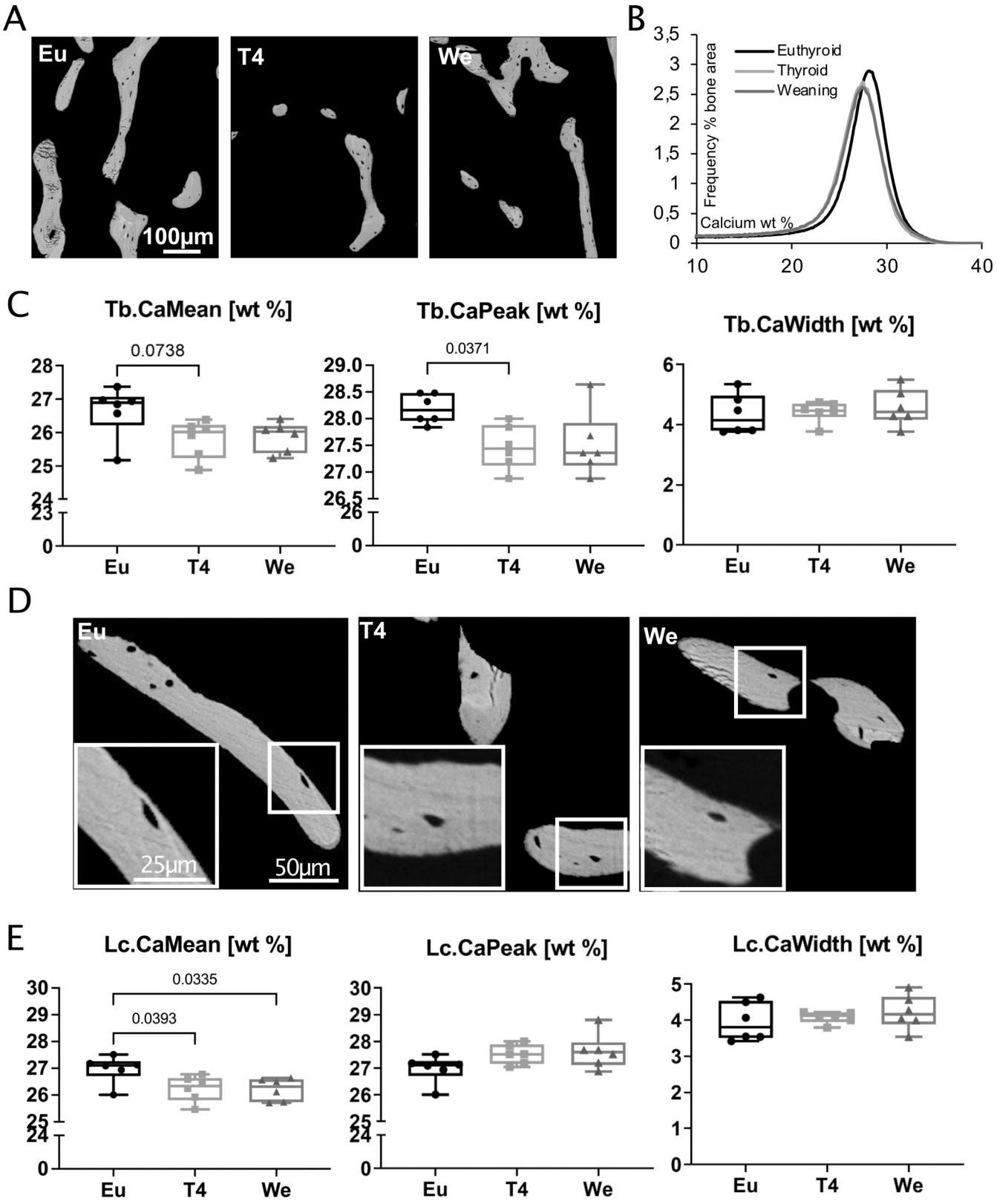

(Figure legend continues on next page.)

15234681, 0, Downloaded from https://asbmr.onlinelibrary.wiley.com/doi/10.1002/jbmr.4736 by Sächsische Landesbibliothek, Wiley Online Library on [05/01/2023]. See the Terms and Conditions (https://onlinelibrary.wiley.com/terms-and-conditions) on Wiley Online Library for rules of use; OA articles are governed by the applicable Creative Commons License

altered global bone mineral density distribution in trabecular bone in response to hyperthyroidism. Additionally, local bone mineral content seems to be controlled by osteocytes, which has been supported by us and others using high-resolution synchrotron determining differential mineralization around the osteocyte lacunae.[36,37] The lower global mineralization degree in combination with the observed osteocyte activity-induced changes may potentially contribute to increased bone fragility in hyperthyroid patients.

Despite its strengths, our study has potential limitations. The mild type of osteocytic osteolysis detected was not reflected by the osteocyte lacunar area but rather shown by other parameters such as higher TRAP activity in osteocytes and a lower mineralization degree around the osteocyte lacunae. A smaller group size as compared to our preliminary analysis (six versus nine mice per group) and the chosen duration for T_4 administration and recovery might explain absence of lacunar area changes. Also, we focused on male mice to reduce the effect of sex-related changes on bone tissue. Parts of our analyses are based on histology, which might result in processing artifacts such as apparent empty lacunae due in 4-µm thin sections. Equal processing of all samples following well established protocols ensures that such influences can be neglected. Additionally, we combined histological analysis with a TUNEL assay to further determine cell death.

In conclusion, our study showed a high bone turnover state in hyperthyroid mice accompanied by a higher TRAP activity in osteocytes. Although the low bone mass recovered in both bone compartments during the weaning period, the initiated osteocytic osteolysis indicated by higher TRAP activity was not reversed as shown by a persistently low mineralization degree around the osteocyte lacunae in the weaning group. Future preclinical studies should address whether osteocytic osteolysis might be more pronounced at different time points during T_4 treatment. Contribution of osteocytes to hyperthyroidism related bone loss are understudied and detailed insights on how thyroid hormones affect the osteocyte network could improve the bone health of hyperthyroid patients with osteoporosis by focusing on osteocytes as therapeutic targets.

Acknowledgments

We thank Sandra Perkovic, Eranston Rajavasthagar and Johannes Krug, Department of Osteology and Biomechanics, Medical University Center Hamburg-Eppendorf, for their excellent technical and imaging assistance. The authors acknowledge the funding by the Fritz Thyssen Foundation under grant no. Az. 10.20.2.042MN and the Elsbeth Bonhoff foundation under grant no. Az.231 to ET, the German Research Foundation (DFG) under grant no. JA2654/1-1 to KJR, the Fund of the Faculty of Medicine from the University Medical Centre Hamburg-Eppendorf to EMW, the DFG under grant no. LA 4945/1-1 and the Technische Universität Dresden (MeDDrive Start) to FL, and the DFG grant under BU2562-10/1 to BB. HH is supported by a postdoctoral fellowship granted by the Alexander von Humboldt foundation. Open Access funding enabled and organized by Projekt DEAL.

Author Contributions

Eva Maria Wölfel: Formal analysis; investigation; methodology; project administration; resources; software; validation; visualization; writing – original draft; writing – review and editing. **Franziska Lademann:** Data curation; formal analysis; funding acquisition; investigation; methodology; project administration; resources; software; validation; visualization; writing – original draft; writing – review and editing. **Haniyeh Hemmatian:** Methodology; project administration; resources; software; visualization; writing – review and editing. **Stéphane Blouin:** Data curation; formal analysis; methodology; resources; software; writing – review and editing. **Phaedra Messmer:** Data curation; methodology; resources; software. **Lorenz Hofbauer:** Supervision; validation; writing – review and editing. **Björn Busse:** Data curation; funding acquisition; methodology; resources; software; supervision; validation; writing – review and editing. **Martina Rauner:** Formal analysis; methodology; project administration; resources; software; supervision; validation; writing – review and editing. **Katharina Jähn-Rickert:** Conceptualization; data curation; funding acquisition; investigation; methodology; resources; supervision; validation; writing – review and editing. **Elena Tsourdi:** Conceptualization; data curation; funding acquisition; investigation; methodology; resources; supervision; validation; writing – review and editing. [Correction added on 2 December 2022 after first online publication: Katharina Jähn-Rickert added to the Author Contributions].

Conflicts Of Interest

ET received research funding from MSD, honoraria for lectures from Amgen, UCB, Shire, Kyowa Kirin, and educational grants from Shire and UCB. MR received honoraria for lectures from Amgen, UCB, Diasorin, and research materials from Novartis, Acceleron, and Regeneron. LCH reports honoraria for advisory boards from Alexion, Amgen, Merck, Radius, Roche, Shire, and UCB to his institution and himself. The remaining authors have nothing to disclose.

Peer Review

The peer review history for this article is available at https://publons.com/publon/10.1002/jbmr.4736.

(Figure legend continued from previous page.)

Fig. 6. Lower global and local trabecular calcium content in T_4-treated mice. (*A*) Representative backscattered electron images show the local distribution of the mineral content in gray scale in the trabecular bone compartment of femurs of all three groups. (*B*) Histograms of calcium weight percentage (wt %) over frequency % of bone area. (*C*) Mean calcium wt % (CaMean), peak position of calcium wt % (CaPeak) and the standard deviation of the histogram curve (CaWidth) as a measurement for mineralization heterogeneity were assessed in trabecular bone (Tb.) of femurs. (*D*) The local mineral content around osteocyte lacunae was determined in trabecular bone and (*E*) the lacunar (Lc.) CaMean, CaPeak, and CaWidth were determined. $n = 6$ each per group. Box plots show median line and the 25th and 75th percentile, the error bars represent the minimum (0th percentile) and the maximum (100th percentile). Individual data points are shown as dots. Statistical analysis was performed using one-way ANOVA with Tukey post hoc test and $p < 0.05$ was considered significant. Eu = euthyroid control group; T4 = hyperthyroid group; We = weaning group.

15234681, 0, Downloaded from https://asbmr.onlinelibrary.wiley.com/doi/10.1002/jbmr.4736 by Sächsische Landesbibliothek, Wiley Online Library on [05/01/2023]. See the Terms and Conditions (https://onlinelibrary.wiley.com/terms-and-conditions) on Wiley Online Library for rules of use; OA articles are governed by the applicable Creative Commons License

Data Availability

All data needed to evaluate the conclusion in the paper are presented in the paper. The datasets generated during and/or analyzed during the current study are not publicly available but are available from the corresponding author upon reasonable request.

References

1. Ebeling PR, Hanh HN, Aleksova J, Vincent AJ, Wong P, Milat F. Secondary osteoporosis. Endocr Rev. 2022;43(2):240-313.
2. Painter SE, Kleerekoper M, Camacho PM. Secondary osteoporosis: a review of the recent evidence. Endocr Pract. 2006;12(4):436-445.
3. Hofbauer LC, Hamann C, Ebeling PR. Approach to the patient with secondary osteoporosis. Eur J Endocrinol. 2010;162(6):1009-1020.
4. Gogakos AI, Duncan Bassett JH, Williams GR. Thyroid and bone. Arch Biochem Biophys. 2010;503(1):129-136. https://doi.org/10.1016/j.abb.2010.06.021.
5. Williams GR, Bassett JHD. Thyroid diseases and bone health. J Endocrinol Invest. 2018;41(1):99-109.
6. Duncan Bassett JH, Williams GR. Role of thyroid hormones in skeletal development and bone maintenance. Endocr Rev. 2016;37(2):135-187.
7. Gouveia CH, Schultz JJ, Bianco AC, Brent GA. Thyroid hormone stimulation of osteocalcin gene expression in ROS 17/2.8 cells is mediated by transcriptional and post-transcriptional mechanisms. J Endocrinol. 2001;170(3):667-675.
8. Varga F, Rumpler M, Luegmayr E, Fratzl-Zelman N, Glantschnig H, Klaushofer K. Triiodothyronine, a regulator of osteoblastic differentiation: depression of histone H4, attenuation of c-fos/c-jun, and induction of osteocalcin expression. Calcif Tissue Int. 1997;61(5):404-411.
9. Banovac K, Koren E. Triiodothyronine stimulates the release of membrane-bound alkaline phosphatase in osteoblastic cells. Calcif Tissue Int. 2000;67(6):460-465.
10. Miura M, Tanaka K, Komatsu Y, et al. A novel interaction between thyroid hormones and 1,25(OH)2D3 in osteoclast formation. Biochem Biophys Res Commun. 2002;291(4):987-994.
11. Lademann F, Tsourdi E, Rijntjes E, et al. Lack of the thyroid hormone transporter Mct8 in osteoblast and osteoclast progenitors increases trabecular bone in male mice. Thyroid. 2020;30(2):329-342.
12. Tsourdi E, Rijntjes E, Köhrle J, Hofbauer LC, Rauner M. Hyperthyroidism and hypothyroidism in male mice and their effects on bone mass, bone turnover, and the Wnt inhibitors sclerostin and dickkopf-1. Endocrinology. 2015;156(10):3517-3527.
13. Tsourdi E, Lademann F, Ominsky MS, et al. Sclerostin blockade and zoledronic acid improve bone mass and strength in male mice with exogenous hyperthyroidism. Endocrinology. 2017;158(11):3765-3777.
14. Buenzli PR, Sims NA. Quantifying the osteocyte network in the human skeleton. Bone. 2015;75:144-150.
15. Plotkin LI, Gortazar AR, Davis HM, et al. Inhibition of osteocyte apoptosis prevents the increase in osteocytic receptor activator of nuclear factor kappa-beta ligand (RANKL) but does not stop bone resorption or the loss of bone induced by unloading. J Biol Chem. 2015;290(31):18934-18942.
16. Milovanovic P, Zimmermann EA, Hahn M, et al. Osteocytic canalicular networks: morphological implications for altered mechanosensitivity. ACS Nano. 2013;7(9):7542-7551.
17. Qing H, Ardeshirpour L, Divieti Pajevic P, et al. Demonstration of osteocytic perilacunar/canalicular remodeling in mice during lactation. J Bone Miner Res. 2012;27(5):1018-1029.
18. Tsourdi E, Jähn K, Rauner M, Busse B, Bonewald LF. Physiological and pathological osteocytic osteolysis. J Musculoskeletal Neuronal Interact. 2018;18(3):292-303.
19. Vahidi G, Rux C, Sherk VD, Heveran CM. Lacunar-canalicular bone remodeling: Impacts on bone quality and tools for assessment. Bone. 2021;143:115663.
20. Monfoulet LE, Rabier B, Dacquin R, et al. Thyroid hormone receptor β mediates thyroid hormone effects on bone remodeling and bone mass. J Bone Miner Res. 2011;26(9):2036-2044.
21. Derkx P, Birkenhäger-Frenkel DH. A thionin stain for visualizing bone cells, mineralizing fronts and cement lines in undecalcified bone sections. Biotech Histochem. 1995;70(2):70-74.
22. Jáuregui EJ, Akil O, Acevedo C, et al. Parallel mechanisms suppress cochlear bone remodeling to protect hearing. Bone. 2016;89:7-15.
23. Busse B, Hahn M, Soltau M, et al. Increased calcium content and inhomogeneity of mineralization render bone toughness in osteoporosis: mineralization, morphology and biomechanics of human single trabeculae. Bone. 2009;45(6):1034-1043.
24. Hemmatian H, Laurent MR, Ghazanfari S, et al. Accuracy and reproducibility of mouse cortical bone microporosity as quantified by desktop microcomputed tomography. PLoS One. 2017;12(8):e0182996.
25. Jähn K, Kelkar S, Zhao H, et al. Osteocytes acidify their microenvironment in response to PTHrP in vitro and in lactating mice in vivo. J Bone Miner Res. 2017;32(8):1761-1772.
26. Halleen JM, Alatalo SL, Suominen H, Cheng S. Tartrate-resistant acid phosphatase 5b: a novel serum marker of bone resorption. J Bone Miner Res. 2000;15(7):1337-1345.
27. Bianco P, Ballanti P, Bonucci E. Tartrate-resistant acid phosphatase activity in rat osteoblasts and osteocytes. Calcif Tissue Int. 1988;43(3):167-171.
28. Bayley TA, Harrison JE, Mcneill KG, John R. Effect of thyrotoxicosis and its treatment on bone mineral and muscle mass. J Clin Endocrinol Metab. 1980;50(5):916-922.
29. Langdahl B, Loft AGR, Eriksen EF, Mosekilde L, Charles P. Bone mass, bone turnover and body composition in former hypothyroid patients receiving replacement therapy. Eur J Endocrinol. 1996;134(6):702-709.
30. Vestergaard P, Mosekilde L. Hyperthyroidism, bone mineral, and fracture risk—a meta-analysis. Thyroid. 2003;13(6):585-593.
31. Cummings S, Nevitt M, Browner W, et al. Risk factors for hip fracture in white women. N Engl J Med. 1995;332(12):767-773.
32. Garnero P, Vassy V, Bertholin A, Riou JP. Markers of bone turnover in hyperthyroidism and the effects of treatment. J Clin Endocrinol Metab. 1994;78(4):955-959.
33. Dole NS, Mazur CM, Acevedo C, et al. Osteocyte-intrinsic TGF-b signaling regulates bone article osteocyte-intrinsic TGF-b signaling regulates bone quality through perilacunar/canalicular remodeling. Cell Rep. 2017;21(9):2585-2596.
34. Tang S, Herber R-P, Ho S, Alliston T. Matrix metalloproteinase-13 is required for osteocytic perilacunar remodeling and maintains bone fracture resistance. J Bone Miner Res. 2012;27(9):1936-1950.
35. Parfitt AM. The cellular basis of bone turnover and bone loss a rebuttal of the osteocytic resorption-bone flow theory. Clin Orthop Relat Res. 1977;127:236-247.
36. Kerschnitzki M, Kollmannsberger P, Burghammer M, et al. Architecture of the osteocyte network correlates with bone material quality. J Bone Miner Res. 2013;28(8):1837-1845.
37. Stachnik K, Warmer M, Mohacsi I, et al. Multimodal X-ray imaging of nanocontainer-treated macrophages and calcium distribution in the perilacunar bone matrix. Sci Rep. 2020;10(1):1784.

15234681, 0, Downloaded from https://asbmr.onlinelibrary.wiley.com/doi/10.1002/jbmr.4736 by Sächsische Landesbibliothek, Wiley Online Library on [05/01/2023]. See the Terms and Conditions (https://onlinelibrary.wiley.com/terms-and-conditions) on Wiley Online Library for rules of use; OA articles are governed by the applicable Creative Commons License